Proceedings of the 38th Chinese Control Conference
July 27-30, 2019, Guangzhou, China

An Improved LSTM Based Sensor Fault Diagnosis Strategy for the Air-cooled Chiller System

Long Gao, Donghui Li, Ding Li, Haiyan Yin

1. School of Electrical and Information Engineering, Tianjin University, Tianjin 300072
E-mail: gao_long@tju.edu.cn

Abstract: In the air-cooled chiller, sensor fault detection and diagnosis (FDD) has great significance to ensure the normal operation of the air conditioning system. Due to the complex system and tiny fault data, traditional methods can't effectively handle this problem. In this paper, an adaptively enhanced Long Short-Term Memory network model (AE-LSTM) is proposed for sensor bias fault detection and diagnosis. Firstly, sensors are divided into several groups by Pearson correlation coefficient. And sensors in each group have the maximum correlation. Subsequently, AE-LSTM is fast trained by normal dataset of sensor groups. In the end, the trained network could properly fit the system of air-cooled chiller. The fault can be diagnosed by the magnitudes of residual which generated by comparing the predicted output of the trained networks with the actual value measured from air-cooled chiller. Detailed experiments and comparisons are made, and the comparison results validate that the AE-LSTM model has a faster and more significant diagnosis performance than the traditional LSTM model.

Key Words: sensor bias fault diagnosis, LSTM, deep learning, Pearson correlation coefficient

1 Introduction

Air-cooled chiller is the core equipment of the refrigeration air conditioning system. According to statistics results supplied by relevant department, air conditioning energy consumption accounts for about 30% of public building energy consumption. When the system return air temperature sensor fault, the system energy consumption increases by 50%. Building consumes more than 40% of the total energy consumption worldwide, and the majority of that is due to Heating, Ventilation, and Air Conditioning system (HVAC) [1]. Thus sensor bias fault detection and diagnosis of air-cooled chiller has great significance for ensuring normal operation and energy saving [2-5].

The sensor bias fault means that the difference between the actual and measured value of the sensor over time. Jeffrey et al. [6-8] proposed fault detection method of air handling units based rule. However, the reliability of the rule method depends on scale of system. If the scale system is small, more sensor bias faults will be difficult to be diagnosed. The sensor fault diagnosis based on Principal Component Analysis (PCA) has been proposed [9-12]. According to the experiment of temperature and humidity sensors, the method was proved to be effective [13]. Whereas PCA method is implemented on assumption in which the refrigeration air conditioning system is a linear system instead of nonlinear system. To solve this problem, Kernel principal component analysis (KPCA) was proposed in [14-17]. However, both the PCA and KPCA methods have more information lost due to the dimensionality reduction and cannot properly consider time correlation of different sensors time series.

As well known, deep learning is capable of automatic and deep mining feature information. As a deep learning model, Recurrent Neural Network (RNN) can properly mine the time correlation of data. LSTM, a variant of the RNN, is developed to solve the problem of gradient disappearance and explosion in the process of gradient back propagation [18]. Based on LSTM unique structure, it plays a vital role in time series prediction. In air conditioning systems, sensor fault detection and diagnosis (FDD) for data center air conditioning system based on LSTM neural network has been proposed [19]. Meanwhile, LSTM consumes a lot of computational costs for training before applying. Greff et al. [20] proposed learning rate, which is very important to achieve good training performance on LSTM. Error will be large, when the learning rate of LSTM is very large or small. Computational time will be large, when the learning rate of LSTM is small.

In this paper, we proposed an adaptively enhanced LSTM model (AE-LSTM) model which can vary error during training by adaptive learning rate for the sensor bias FDD of air-cooled chiller. Firstly, sensors dataset of air-cooled chiller are divided into several groups by Pearson correlation coefficient. Sensors in each group have the maximum similarity. Secondly, normal dataset from sensor groups is used to train the AE-LSTM model. Finally, the fault can be identified by the magnitudes of residual which generated by comparing the output of the trained networks with the actual value measured from the air-cooled chiller. The experimental results show that the AE-LSTM model brings faster and significant diagnosis performance than traditional method.

2 AE-LSTM

The AE-LSTM model is composed with traditional LSTM and adaptively enhanced (AE) module. It can vary error which generated in the training process of air-cooled chiller by adaptive learning rate. In order to speed up the training process, the learning rate should be as large as possible at an early stage. At the same time, the learning rate should be appropriately reduced in the later stage. The adaptively enhanced module can adaptively set the learning rate in each iteration. Thus the AE-LSTM model has the faster and stable performance.

*This work is supported by National Natural Science Foundation (NNSF) of China under Grant No. 61873180.

2.1 LSTM

2.1.1 Traditional RNN

Traditional RNN which has a recursive structure could pass information flow from the previous state to the current state. [21]. Thus it plays a vital role in time series prediction [22-23]. The structure of traditional RNN is shown in Fig. 1.

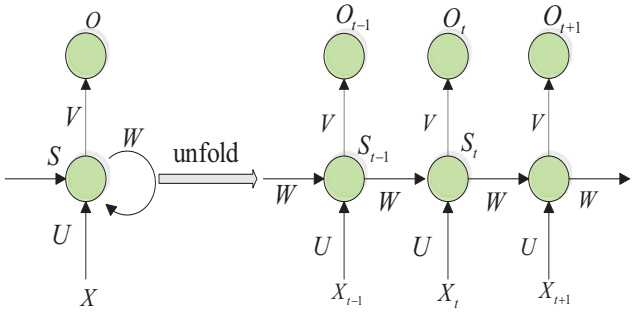

Fig. 1: The structure of traditional RNN

Supposing that the input and output sequence are described in $X=(x_1,x_2,\ldots,x_N)$ and $Y=(y_1,y_2,\ldots,y_N)$ respectively, the traditional RNN is computed as follows:

$$s_t = f(W_{xh}x_t + W_{hh}h_{t-1} + b_h) \quad (1)$$

$$o_t = g(W_{ho}s_t + b_o) \quad (2)$$

where W_{xh}, W_{hh} and W_{ho} are the input weight matrix, recurrent weight matrix and output weight matrix. b_h and b_o are hidden bias and output bias. $f(\cdot)$ and $g(\cdot)$ are the activation functions of hidden layer and output layer.

2.1.2 LSTM

LSTM, a variant of RNN, solves the problem of gradient disappearance and explosion in the process of gradient back propagation. The key to LSTM is LSTM cell which can decide whether to maintain state information [24]. The structure of LSTM cell is shown in Fig. 2.

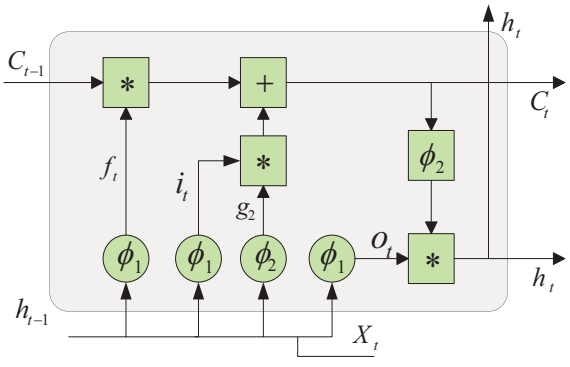

Fig. 2: LSTM cell

LSTM cell contain input gate, forget gate and output gate. The input gate is used to decide the input information to save the state of unit. The forget gate is used to decide the state of unit at the last time. The output gate is used to decide the output of LSTM cell. Outputs c_t and h_t are recurrently connected to the inputs of block. The LSTM block with forward propagation is computed as follows:

$$f_t = \sigma(W_f * [h_{t-1}, x_t] + b_f) \quad (3)$$

$$i_t = \sigma(W_i * [h_{t-1}, x_t] + b_i) \quad (4)$$

$$g_2 = \tanh(W_c * [h_{t-1}, x_t] + b_c) \quad (5)$$

$$c_t = f_t * c_{t-1} + i_t * g_2 \quad (6)$$

$$o_t = \sigma(W_o * [h_{t-1}, x_t] + b_o) \quad (7)$$

$$h_t = o_t * \tanh(c_t) \quad (8)$$

The formulas (3), (4) and (5) are forget gate, input gate and output gate respectively. W_f, W_i and W_c are the weights of forget gate, input gate and output gate respectively. $\sigma(\cdot)$ and $\tanh(\cdot)$ are the sigmoid function and hyperbolic tangent.

2.2 Structure of AE-LSTM

The structure of AE-LSTM model is shown in Fig. 4. Greff et al. [3] proposed that learning rate is the most important hyper parameter in the training process of LSTM. In the process of LSTM back propagation, the error will be increasing, when the learning rate of LSTM is very large or small. Computational time will be increasing, when the learning rate of LSTM is small. AE module can adaptively vary error of back propagation and reduce the computational time by adaptively learning rate. The adaptive learning rate is computed as follows:

$$\eta_1 = \eta(1+\alpha e^{-\lambda d}) \quad (9)$$

where d is the number of iteration, α and λ respectively denote the coefficient of iteration, η is the initial learning rate, η_1 is the adaptive learning rate. When the initial learning rate is 0.0005, the possible curve of learning rate is illustrated in Fig. 3.

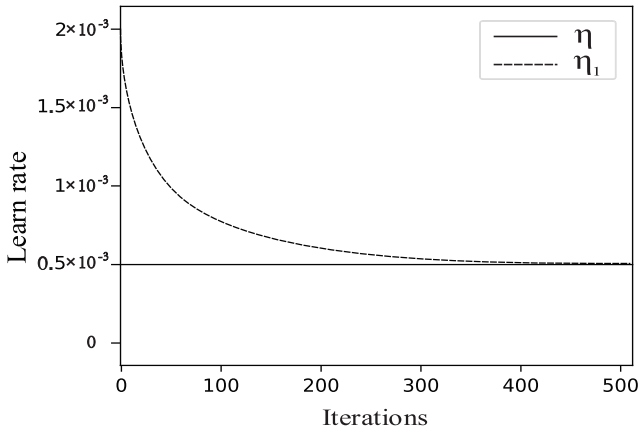

Fig. 3: The curve of learning rate

In back propagation of AE-LSTM, the error can be varied by adaptive learning rate. The weights of W_f, W_i, W_c and W_o are varied as follows:

$$W_f' = W_f - \eta' \Delta W \quad (10)$$

$$W_i' = W_i - \eta' \Delta W \quad (11)$$

$$W_c' = W_c - \eta' \Delta W \quad (12)$$

$$W_o' = W_o - \eta' \Delta W \quad (13)$$

where W_f' , W_i' , W_c' and W_o' represent the LSTM weights after updating, ΔW represent the error in current iteration and η' is adaptive learning rate.

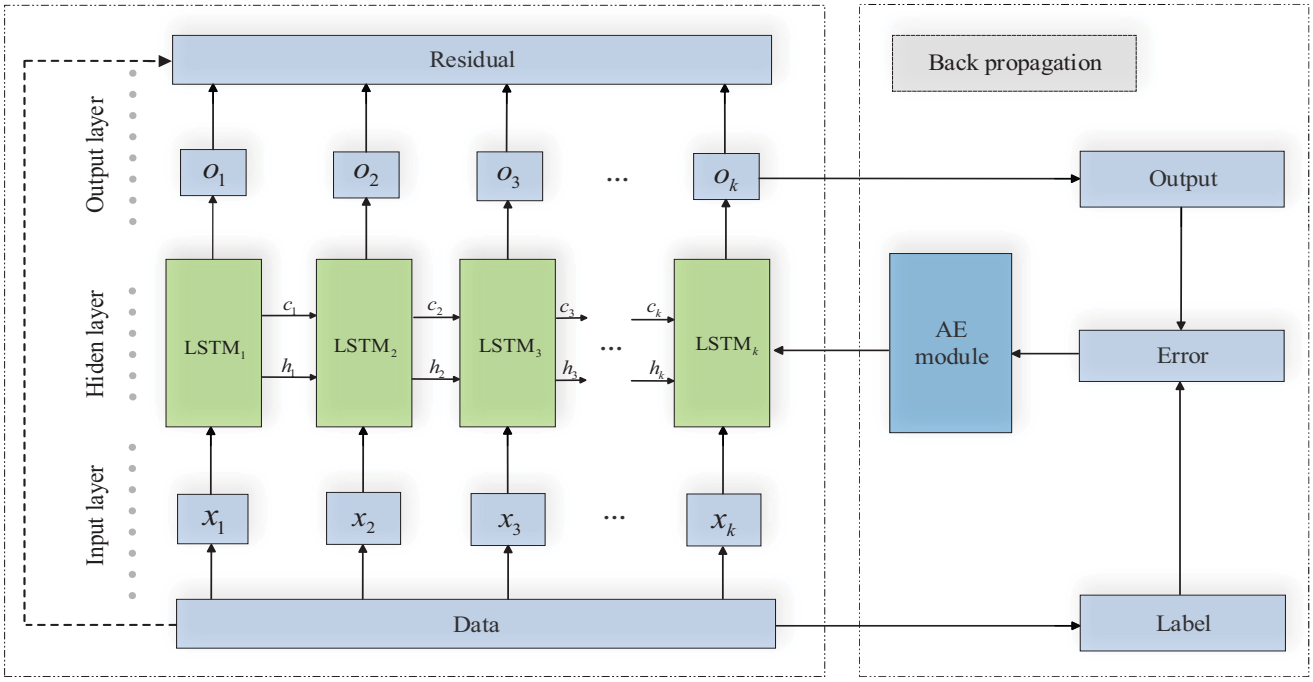

Fig. 4: The structure of AE-LSTM model

3 Experimental verification

Experiments are run on Ubuntu 14.04 with Intel(R) Xeon(R)E5-2690 32.60GHz CPU, Nvidia Tesla K40c 12GB GPU, 256GB RAM and 8TB hard disk.

The AE-LSTM and LSTM models are completed by Python 3.6 with tensorflow 1.2.1. During the experiment, the models have the same hyperparameters, such as learning rate, batch size, etc.

3.1 Sensors correlation analysis

The refrigeration system is a strong coupling system. For example, the output parameters of compressor, such as enthalpy, affect the parameters of condenser. Conversely, the condensing pressure of the condenser causes varies the parameters such as compressor power.

The output parameter of condenser, such as the condensing pressure and flow rate, varies the parameters such as the flow rate of the electronic expansion valve and the value of the outlet enthalpy. Conversely, the flow of the expansion valve affects the parameters such as the condensing pressure and the condensing temperature.

The output parameters of electronic expansion valve, such as enthalpy and flow, affect the evaporation pressure, evaporation temperature and outlet enthalpy of the evaporator. Conversely, the evaporation pressure of the evaporator valve also varies parameters of the electronic expansion such as outlet enthalpy and flow rate. Coupling structure of refrigeration system is shown in Fig. 5.

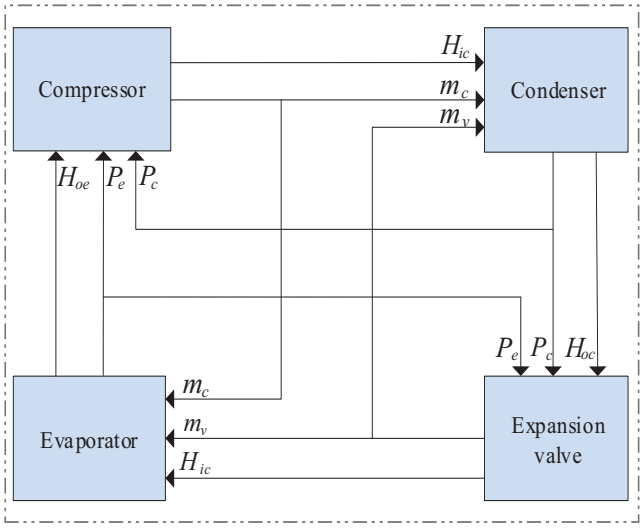

Fig. 5: Coupling structure of refrigeration system

As shown in Fig. 5, H_{oe} , H_{ic} , H_{oc} and H_{ic} represent the output enthalpy of evaporator, compressor, condenser and expansion valve. m_v and m_c represent the expansion valve mass flow and compressor mass flow. P_c and P_e represent the condensing pressure and evaporation pressure.

In this article, we diagnose fault of the seven temperature sensors T(n) (n=1,…,7) and four pressure sensors P(n)

(n=1,…,4) of air-cooled chiller. The experimental data are acquired from the device in Tianjin University. And the descriptions of the measured variables are listed in Table 1.

Table 1: The descriptions of the measured variables

Sensor	Description	Unit
T1	Compressor suction temperature	℃
T2	Compressor exhaust temperature	℃
T3	Condenser outlet temperature	℃
T4	Refrigerant temperature before throttling	℃
T5	Refrigerant temperature after throttling	℃
T6	Evaporator inlet water temperature	℃
T7	Evaporator outlet water temperature	℃
P1	Compressor suction pressure	MPa
P2	Compressor discharge pressure	MPa
P3	Inlet pressure of the throttle device	MPa
P4	Outlet pressure of the throttle device	MPa

Compressor, condenser, evaporator and expansion valve interact with each other through energy transfer. According to the strong coupling relationship between different sensors, the value of any sensor can be predicted from the values of other sensors. However, the correlation among sensors is different, and it is better to choose the higher correlated sensors to predict each other. Pearson's correlation coefficient is employed to select the higher correlated sensors of air-cooled chiller as described in Eq. (16).

$$r_{xy} = \frac{\sum_{i=1}^{n}(x_i-\bar{x})(y_i-\bar{y})}{\sqrt{\sum_{i=1}^{n}(x_i-\bar{x})^2}\sqrt{\sum_{i=1}^{n}(y_i-\bar{y})^2}} \tag{16}$$

where $\bar{x}$ and $\bar{y}$ are the mean of x and y.

According to the Pearson correlation coefficient, sensors of air-cooled chiller are divided into several groups. Correlation coefficient of temperature sensors are listed in Table 2.

Table 2: Correlation coefficient of temperature sensors

	T1	T2	T3	T4	T5	T6	T7
T1	1	-0.13	-0.21	-0.18	0.79	0.99	0.99
T2	-0.13	1	0.62	0.63	0.92	-0.13	-0.27
T3	-0.21	0.62	1	0.98	0.20	-0.18	-0.29
T4	-0.18	0.63	0.98	1	0.22	-0.19	-0.19
T5	0.79	0.92	0.20	0.22	1	0.80	0.80
T6	0.99	-0.13	-0.18	-0.19	0.80	1	0.99
T7	0.99	-0.27	-0.29	-0.19	0.80	0.99	1

As illustrated in Table 2, temperature sensors can be divided three groups: T1, T6, T7 and T2, T5 and T3, T4. The sensors of each group have the higher correlation.

The correlation coefficient of pressure sensors are listed in Table 3. In the similar way, it can be divided two groups: P1, P2 and P3, P4. The sensors of each group have display high correlation.

Table 3: Correlation coefficient of pressure sensors

	P1	P2	P3	P4
P1	1	0.98	0.134	0.36
P2	0.98	1	0.21	0.37
P3	0.134	0.21	1	0.92
P4	0.36	0.37	0.92	1

Hence temperature and pressure sensors have been divided five groups by using the Person correlation coefficient. Sensors fault can be diagnosed in each group by LSTM and AE-LSTM models.

3.2 Comparison of LSTM and AE-LSTM

The sensor bias fault means that the difference between the actual and measured value of air-cooled chiller sensor over time. The actual value represented by the black line. The value of sensor becomes larger and tends to stabilize over time. We assume that only one sensor has failed. The biased fault of T6 is shown in Fig. 6.

Table 4: The computational time of different models (s)

The number of hidden nodes	LSTM	AE-LSTM
16	16.32	15.54
32	17.24	16.35
64	17.99	16.89
128	19.89	18.11
256	22.65	19.88

By changing the number of hidden nodes in LSTM and AE-LSTM cell, the computational time can be listed in Table 4. It can be seen from the results in Table 4, when the same loss is reached, the computational time of AE-LSTM is less than LSTM model. As the number of hidden nodes increases, the amount of calculation will be greatly reduced. When the number of hidden nodes is 16, the computational time achieve 4.78% improvement on AE-LSTM. When the number of hidden nodes is 256, the computational time achieve 12.23% improvement on AE-LSTM. As the number of hidden nodes grows, a growing number of times are saved.

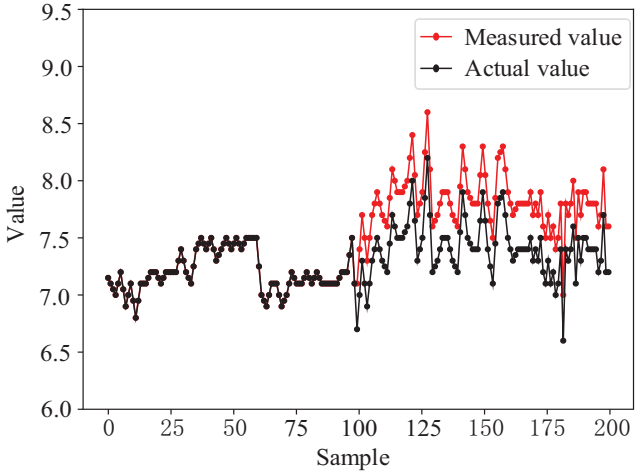

Fig. 6: The biased fault of T6

Fig. 7 shows the loss varying in back propagation. When the epoch of training is big enough, the value of loss can very small. When the sensor is faulty, residual which generated by comparing the output of the trained networks with the actual measured value of the air-cooled chiller can be varies. By comparing the value of residual, AE-LSTM model can diagnose the fault.

In the case of the T6 fault, the residual of corresponding group is shown in Fig. 8. When the sensor does not fault, the residual of sensors are tiny. The sensor fault appears at the hundredth sample point. At the same time, due to the high correlation, the residual of T1, T6 and T7 increased together. By comparing the value of residual, we can see that the residual of T6 is the biggest. Thus, the biased fault of T6 diagnosed.

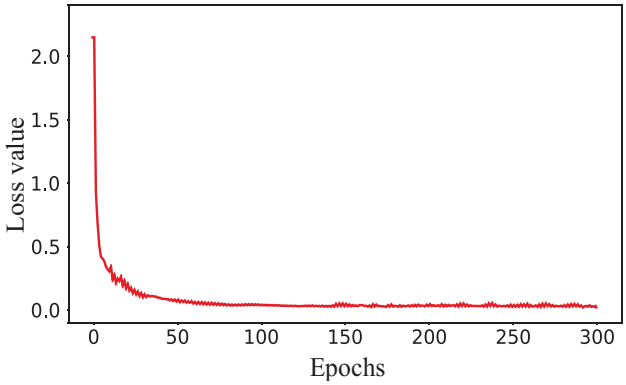

Fig. 7: The loss varies in back propagation

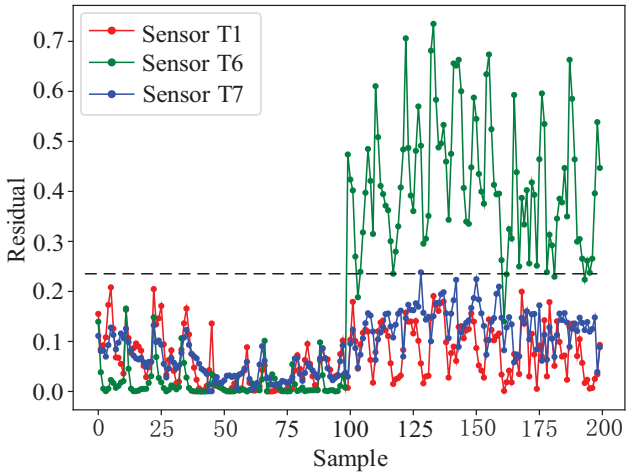

Fig. 8: The residual of corresponding group

When the sensor P2 is faulty, the residual of corresponding group is shown in Fig. 9. The sensor P2 fault appears at the hundredth sample point. The residual of P1, P2 increased at the same time. By comparing the value of residual, P2 brings significant residual than P1. In the same situation, the sensor P2 is faulty.

The residual of AE-LSTM and LSTM models are shown in Fig. 10. In the case of the sensor is faulty, the average residual of AE-LSTM is about 0.49 and LSTM is about 0.31. The residual of AE-LSTM outperforms LSTM model. Thus, AE-LSTM brings more sensitive performance.

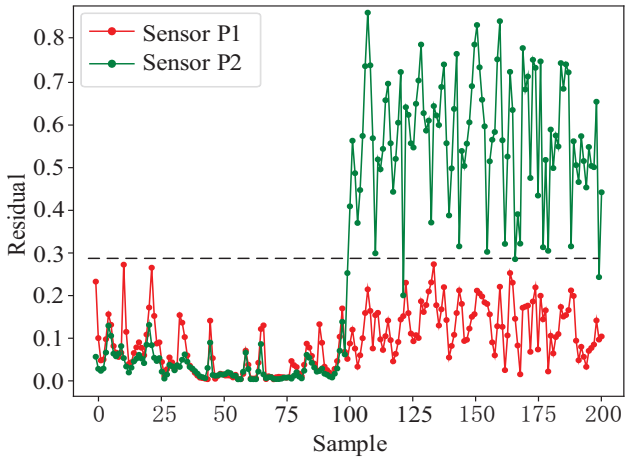

Fig. 9: The residual of corresponding group

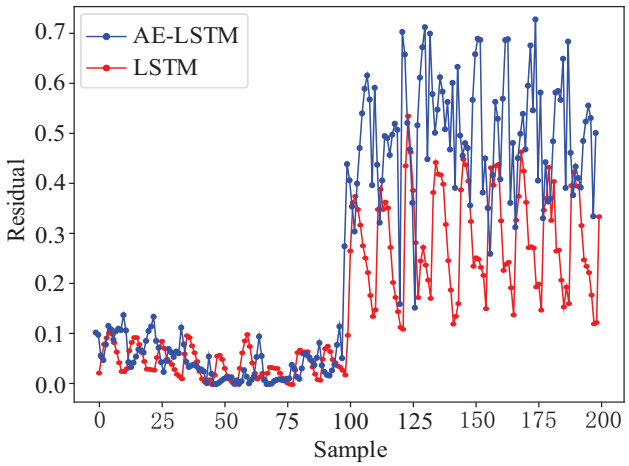

Fig. 10: The residual of different models

4 Conclusion

In this paper, AE-LSTM model which can vary error by adaptive learning rate for the sensor bias fault diagnosis of air-cooled chiller has been proposed. AE module can adaptively vary error of back propagation and reduce the computational time by adaptive learning rate. The experimental results show that the AE-LSTM model brings significant performance than traditional method.

In future work, AE-LSTM model will be applied to other refrigeration air conditioning system to verify generalization and will be verified residual varies when multiple sensors fault.

References

[1] G. Mantovani and L. Ferrarini, Temperature control of a commercial building with model predictive control techniques, *IEEE Transactions on Industrial Electronics*, 62(4), 2651–2660, 2015.

[2] O. Y. Odufuwa, K. Kusakana and B. P. Numbi, Review of Optimal Energy Management Applied on Ice Thermal Energy Storage for an Air Conditioning System in Commercial Buildings, in *2018 Open Innovations Conference (OI)*, 2018, 286-293.

[3] M. Ehyaei, A. Mozafari, A. Ahmadi, P. Esmaili, M. Shayesteh, M. Sarkhosh and I. Dincer, Potential use of cold thermal energy storage systems for better efficiency and cost effectiveness, *Energy and Buildings*, 42(12), 2296-2303, 2010.

[4] J. Nowotny, J. Dodson, S. Fiechter, T. Gür, B. Kennedy, W. Macyk, T. Bak, W. Sigmund, M. Yamawaki and K. Rahman, Towards global sustainability: Education on environmentally clean energy technologies, *Renewable and Sustainable Energy Reviews*, 2018, 2541-2551.

[5] M. Wiggins, J. Brodrick, HVAC fault detection, *ASHRAE Journal*, 2012(2): 78-80

[6] Schein J, Bushby S T , Castro N S , et al. A rule-based fault detection method for air handling units, *Energy and Buildings*, 38(12):1485-1492, 2006.

[7] M. Zhou and T. Wang, Fault diagnosis of power transformer based on association rules gained by rough set, *In 2010 The 2nd International Conference on Computer and Automation Engineering (ICCAE)*, Singapore, 2010, pp. 123-126.

[8] Z. Zhou, Z. Feng, C. Hu, F. Zhao, Y. Zhang and G. Hu, Fault detection based on belief rule base with online updating attribute weight, *In 2017 32nd Youth Academic Annual Conference of Chinese Association of Automation (YAC)*, Hefei, 2017, 272-276.

[9] L. Zhang, M. Huang and D. Hong, A fault detection approach for aero-engines based on PCA, *In 2009 8th International Conference on Reliability, Maintainability and Safety*, Chengdu, 2009, 874-878.

[10] C. Wang, J. Hu and C. Wen, Multi-level PCA and its application in fault diagnosis, *In the 26th Chinese Control and Decision Conference (2014 CCDC)*, Changsha, 2014, 2810-2814.

[11] N. Bhattacharjee and B. K. Roy, Fault detection and isolation of a two non-interacting tanks system using partial PCA, *In 2010 International Conference on Industrial Electronics, Control and Robotics*, Orissa, 2010, 137-141.

[12] K. Jafarian, M. Darjani and Z. Honarkar, Vibration analysis for fault detection of automobile engine using PCA technique, *In 2016 4th International Conference on Control, Instrumentation, and Automation (ICCIA)*, Qazvin, 2016, 372-376.

[13] D. Li, L. Wang. S. wang. Fault Diagnosis of Sensors in Air-Conditioning System Based on PCA Method, *transactions of china electro technical society*, 23(6):130-136, 2008.

[14] X. Zhang, W. W. Yan, X. Zhao, H. H. Shao, Nonlinear online process monitoring and fault diagnosis of condenser based on kernel PCA plus FDA, *journal of southeast university*, 2007, 23(1), 51-56

[15] Y. Gao, S. Wang and Z. Liu, Automatic Fault Detection and Diagnosis for Sensor Based on KPCA, *In 2009 Second International Symposium on Computational Intelligence and Design*, 2009, 135-138.

[16] N. Zhang, X. Gao, Y. Li and P. Wang, Fault detection of chiller based on improved KPCA, *In 2016 Chinese Control and Decision Conference (CCDC)*, 2016, 2951-2955.

[17] J. Ni, C. Zhang and S. X. Yang, An Adaptive Approach Based on KPCA and SVM for Real-Time Fault Diagnosis of HVCBs, *IEEE Transactions on Power Delivery*, 26(3), 1960-1971, 2011.

[18] Sepp Hochreiter and Jurgen Schmidhuber. Long shorter memory. *Neural computation*, 9(8), 1735 – 1780, 1997.

[19] L. Y. Wang, B. Wu, Z. M. Du, X. Q. Jin, Sensor Fault Detection and Diagnosis for Data Center Air Conditioning System Based on LSTM Neural Network, *Journal of Chemical Industry and Engineering*, 1-9, 2018.

[20] K. Greff, R. K. Srivastava, J. Koutník, B. R. Steunebrink and J. Schmidhuber, LSTM: A Search Space Odyssey, *IEEE Transactions on Neural Networks and Learning Systems*, 28(10), 2222-2232, 2017.

[21] H. Shao, Delay-Dependent Stability for Recurrent Neural Networks With Time-Varying Delays, *IEEE Transactions on Neural Networks*, 19(9), 1647-1651, 2008.

[22] Gherrity, A learning algorithm for analog, fully recurrent neural networks, *In International 1989 Joint Conference on Neural Networks*, Washington, DC, USA, 1989, 643-644 vol.1.

[23] Q. Song, Y. Wu and Y. C. Soh, Robust Adaptive Gradient-Descent Training Algorithm for Recurrent Neural Networks in Discrete Time Domain, *IEEE Transactions on Neural Networks*, 19(11), 1841-1853, 2008.

[24] Felix A Gers, Jurgen Schmidhuber, and Fred Cummins. Learning to forget: Continual prediction with lstm. *Neural computation*, 12(10), 2451 – 2471, 2000.